Biochimica et Biophysica Acta, 1027 (1990) 163–171
Elsevier

BBAMEM 74958

Biophysical correlates of lysophosphatidylcholine- and ethanol-mediated shape transformation and hemolysis of human erythrocytes. Membrane viscoelasticity and NMR measurement

Lang-Ming Chi [1], Wen-guey Wu [1], Kuo-Li Paul Sung [2,*] and Shu Chien [2,*]

[1] *Institute of Life Sciences, National Tsing Hua University, Hsinchu, Taiwan and* [2] *Institute of Biomedical Sciences, Academia Sinica, Taipei, Taiwan (China)*

(Received 3 January 1990)

Key words: Hemolysis; Erythrocyte shape; Micropipette aspiration; NMR; Ethanol; Lysophosphatidylcholine; Membrane viscoelasticity

The effects of monopalmitoylphosphatidylcholine (MPPC or lysophosphatidylcholine) and a series of short-chain primary alcohols (ethanol, 1-butanol and 1-hexanol) on cell shape, hemolysis, viscoelastic properties and membrane lipid packing of human red blood cells (RBCs) were studied. For MPPC, the effective membrane concentration to induce the formation of stage 3 echinocytes ($8 \cdot 10^6$ molecules per cell) was one order of magnitude lower than that needed to induce 50% hemolysis ($7 \cdot 10^7$ molecules per cell). In contrast, short-chain alcohols induced both shape changes and hemolysis within close concentration range ($2.5 \cdot 10^8$ to $3.5 \cdot 10^8$ molecules per cell). Viscoelastic properties of the RBCs were studied by micropipette aspiration and correlated with shape change. Ethanol-treated RBCs showed a decrease in membrane elastic modulus and an increase in membrane viscosity in the recovery phase at the early stage of shape change. MPPC-treated cells showed the same type of viscoelastic changes, but these were not observed until the formation of stage 2 echinocytes. High-resolution solid-state ^{13}C nuclear magnetic resonance technique was applied to study membrane lipid packing in the ghost membrane by following the chemical shift of hydrocarbon chains. Both MPPC and ethanol caused the ^{13}C-NMR chemical shift to move upfield, indicating that membrane lipids were expanded due to the intercalation of these exogenous molecules. Using data obtained from model compounds, we convert values of chemical shift into a lipid packing parameter, i.e., number of *gauche* bonds for fatty acyl hydrocarbon chains. Approximately 10^8 interacting molecules per cell are required to induce a detectable change of lipid packing by both MPPC and ethanol. The results indicate that homolysis occurs at a smaller surface area for MPPC- than ethanol-treated RBCs. Our findings suggest that progressive changes in the molecular packing in the membrane lead eventually to hemolysis, but the mode responsible for shape transformation varies with these amphipaths.

Introduction

It is well established that the red blood cell (RBC) can easily undergo shape transformation in vitro in response to a variety of chemical agents [1–6]. Treatment of fresh RBCs with lysophosphatidylcholine [2–4,7,8], anionic (sodium alkyl sulphates) amphiphile [5] or ethanol [9] can lead to crenation, i.e., the formation of echinocytes. These shape changes occur rapidly and are reversible prior to the formation of spherocytes. There is evidence that the erythrocyte shape change corresponds quantitatively to the number of molecules

* Present address: Department of AMES-Bioengineering, R-012, University of California, San Diego, La Jolla, CA 92093-0412, U.S.A.

Abbreviations: RBC, red blood cell; MPPC, monopalmitoylphosphatidylcholine; DPPC, dipalmitoylphosphatidylcholine; MI, morphological index; NMR, nuclear magnetic resonance; CP/MAS, cross polarization/magic angle spinning; TMS, tetramethylsilane.

Correspondence: W. Wu, Institute of Life Sciences, National Tsing Hua University, Hsinchu, Taiwan 30043, China.
Correspondence: S. Chien, Department of AMES-Bioengineering, R-012, University of California, San Diego, La Jolla, CA 92093-0412, U.S.A.

incorporated as a result of their preferential intercalation into one hemileaflet of the membrane to expand its area, thus altering membrane curvature and hence cell shape [1–4,10]. At sufficiently high concentrations these exogenous amphipathic molecules cause hemolysis by creating holes in the RBC membranes [11–13]. The interactions of amphipathic molecules with RBC membranes are probably different during shape transformation and hemolysis, although they may both result from the intercalation of molecules into the cell membrane. Biophysical properties of cell membrane such as viscoelasticity and lipid packing should reflect changes of its molecular organization and biochemical composition [14,15]. Therefore, it would be valuable to examine the effects of these molecules on the biophysical properties of RBC membranes at various stages of shape transformation and hemolysis.

Among the available physical techniques for studying cell membrane properties, micropipette aspiration and nuclear magnetic resonance (NMR) could provide useful information on membrane deformability [14–17] and lipid lateral packing [18–20], respectively. It has been shown that shape-transformed human RBCs exhibit increased resistance to membrane deformation [15,16]. The formation of spicules on an RBC results in regional variations of viscoelastic properties on the membrane. The present study was designed to elucidate the mechanisms of morphological and biophysical changes of RBC membrane in response to different amphipathic compounds. The results have provided new insights into the biophysical basis of RBC shape transformation and hemolysis.

Materials and Methods

Monopalmitoylphosphatidylcholine (MPPC, or lysophosphatidylcholine) was purchased from Sigma Chemicals, St Louis, MO. Dipalmitoylphosphatidylcholine (DPPC) was purchased from Avanti Polar Lipids, Inc., Birmingham, AL. Ethanol, 1-butanol, 1-hexanol and other chemicals were purchased from Merck, Rahway, NJ. All of the chemicals are reagent grade.

Red blood cell preparation

Blood was obtained from healthy adult volunteers by venipuncture and collected into 3.2% sodium citrate, with a blood : sodium citrate ratio of 9 : 1 (v/v). RBCs were separated from plasma and buffy coat by centrifugation at 3000 rpm (IEC, Centra-4B) for 5 min, and washed three times with 4 volumes of 150 mM NaCl and once with P_i buffer (138 mM NaCl, 5 mM KCl, 6.1 mM Na_2HPO_4, 1.4 mM NaH_2PO_4, 1 mM $MgSO_4$, 5 mM glucose (pH 7.4)) or a BSA-Tris buffer (150 mM NaCl, 0.25% BSA, 0.1% EDTA (pH 7.4)). After removal of the supernatant, the packed RBCs were suspended with the P_i or BSA-Tris buffer to the desired hematocrit and incubated with the appropriate reagent for 2–3 h. All experiments were performed at room temperature. The cells stored at 4°C were used within 6 h after sampled.

Morphology and hemolysis detection

Suspensions of RBCs in buffer, range in hematocrit from 0.01 to 50%, were incubated with different concentrations of MPPC or alcohols in the P_i buffer. At time intervals specified in the figure legends, one drop (≈ 30 μl) of the cell suspension was removed for morphological study. At the same time, 1 ml of cell suspension was pipetted to assay for hemolysis.

To stop the shape change process and to preclude the 'glass effect', RBCs were fixed at a hematocrit below 0.5% in 0.5% glutaraldehyde in 150 mM NaCl for 20 min. Cells were moisturized in 40% glycerol and viewed under 1000× phase contrast microscope. Cell morphology was graded on a scale of +1 to +5 for echinocytes and −1 to −4 for stomatocytes based on the nomenclature of Bessis [23]. The average score of 100 RBCs in several fields was taken as the morphological index (MI). For the assessment of hemolysis, the RBC suspensions were centrifuged at 4000 rpm (Eppendorf, Centrifuge 5415) for 5 min and the optical density of the supernatant was determined at 540 nm. Reference values were obtained from the same amount of RBCs in distilled water (100% hemolysis) and in reagent-free buffer (0% hemolysis).

Fixed RBCs by 0.5% glutaraldehyde in 150 mM NaCl for 1 h at 4°C were also prepared for scanning electron microscopy (Hitachi, S-2300) by washing four times with distilled water, freeze-drying 2.5 μl of a 1% hematocrit suspension on a glassslip, and sputter coating with gold before viewing.

Control experiments were performed to test the possible effect of ATP depletion during the experimental time period on both the morphology and hemolysis of RBC. In this case, RBCs were incubated at 20% hematocrit with 6 mM iodoacetamide and 10 mM inosine in the P_i buffer for 30 min to effect rapid ATP depletion [3]. Then the cells were washed three times with the P_i buffer, prior to incubation with MPPC or alcohols. There is no significant change for both the morphology and hemolysis of RBC induced when amphipaths were studied in the presence or absence of ATP.

Estimation of amphipath concentration in the cell membrane

It is reasonable to assume that a certain critical concentration of amphipath in the membranes is needed to achieve morphological changes. This membrane concentration (C_m) is given as the number of molecules in the membrane (N_m) per unit membrane volume (V_m).

The partition coefficient (K_p) of the amphipath between membrane and buffer is defined as

$$K_p = C_m/C_b = (N_m/V_m)/(N_b/V_b) \quad (1)$$

where C_b and N_b are the concentration and the number of molecules of the amphipath in the buffer medium, respectively, and V_b is the volume of the buffer. Rearrangement of Eqn. 1 yields

$$V_b/V_m = [K_p/(N_m/V_m)](N_t/V_m) - K_p \quad (2)$$

By plotting V_b/V_m against N_t/V_m, one can estimate K_p for the y intercept and then N_m/V_m from the inverse of the slope [24]. Once the partition coefficient is known, one may use the following equation to calculate the concentration in the membrane (C_m).

$$C_m = \frac{C_i \cdot V_t \cdot K_p}{V + (V_m \cdot K_p)} \quad (3)$$

where C_i is initial amphipathic concentration in aqueous solution and V_t is the total volume of aqueous solution: $V_t \cong V_b + V_m$. The following numerical values [25–27] were used for the calculations: $5.2 \cdot 10^{-13}$ g lipid per ghost; $5.7 \cdot 10^{-13}$ g protein per ghost; 10^{10} cells per ml packed RBC; $6 \cdot 10^9$ ghost cells per ml packed ghost; K_p(ethanol) = 0.14; K_p(butanol) = 1.5; K_p(hexanol) = 13; and K_p(MPPC) = $7.25 \cdot 10^4$.

Measurements of viscoelasticity of RBC by micropipette aspiration

RBCs were washed and resuspended to 0.01% hematocrit in BSA-Tris buffer with 1% human plasma for preventing the attachment of cells to the glass slide. The suspension was transferred to a chamber mounted on an inverted phase-contrast microscope for measurement of viscoelasticity of single cell by micropipette aspiration. BSA is known to affect the MPPC uptake of RBC [2], but it is needed for in the micropipette measurement. We have made concentration correction for 0.01% hematocrit according to the shape change curves with and without BSA; the correction factor is in the range of 180 ± 30-fold which is comparable to that in a previous study [2] if the effect of hematocrit is taken into account. Although possible deviation of the correction factor might change the presently determined MPPC membrane concentration, it will not affect our conclusion on the correlation between membrane viscoelasticity and shape change of RBCs. Morphology of RBCs used for micropipette aspiration was also measured during experiments and the results correspond well to the results shown in Fig. 6. All the viscoelasticity data are reported after normalization with the control results of the normal (untreated) cells studied on the same day.

Micropipettes with radii (R_p) of 0.4 to 0.8 μm were used to study the viscoelastic properties of the RBC membrane before and after amphipath treatment. The methodology has been described in detail by Chien et al. [28], who showed that the deformation entry of the erythrocyte into the micropipette in response to a step aspiration pressure (ΔP) exhibits a two-phase behavior. After an initial rapid phase (phase I) of deformation, there is a continuous, slower phase (phase II) with the final maximum steady-state deformation (D_{pm}) attained within a 20-s period of observation. The membrane elastic modulus is calculated from the stress-strain relationship between $(\Delta P)/R_p$ and D_{pm}/R_p. When the aspiration pressure is removed, the deformed erythrocyte segment in the micropipette decreases in length with time, and there is a single phase of relaxation leading to the complete recovery of cell shape (recovery phase). The membrane viscosity of the various phases is calculated as the product of the time constant of the response and the membrane elastic modulus. There was no significant change of the membrane viscosity values of deformation phases I and II for RBCs treated with MPPC and ethanol. Therefore, only the membrane viscosity in recovery and the elastic modulus are reported here.

Measurements of lipid packing of RBC membranes by CP/MAS ^{13}C-NMR

Unsealed RBC ghost membranes were prepared by lyzing the well-washed RBCs with 5 mM sodium phosphate, pH 8.0 (5P8) at 4° C and centrifuged at 22 000 × g for 10 min [29]. The pellet was washed with the same buffer until it was white. The packed white unsealed-ghosts were condensed by centrifugation at $3 \cdot 10^5 \times g$ at 4° C for 5 to 6 h. The lowest pellet with yellow-colored membranes (condensed unsealed ghost) was collected and weighed. A known amount of either MPPC or ethanol was then added to the condensed ghost membrane in the spinner to a total volume of 300 μl. After 1 h incubation and stirring by vortex at room temperature, the spinner was used for CP/MAS ^{13}C-NMR detection. Ghost membrane concentrations were estimated by protein content assayed by the Lowry method. Membrane concentrations of the added amphipath (number of either MPPC or ethanol molecules per ghost) were calculated according to Eqn. 3 by the known partition coefficient, total volume, and ghost membrane concentration [30].

The ^{13}C spectra of ghost membrane and synthetic dipalmitoylphosphatidylcholine dispersions were obtained by combination of CP/MAS approach [31,33] and proton decoupling, which were performed on a Brüker MSL-200 FT NMR spectrometer in conjunction with an Andrew type magic angle spinning probe. The spinner was made of ZrO_2 or Al_2O_3 with an internal volume of 350 μl and was spun with compressed air at 1.2–1.5 KHz. Adamantane was utilized to match the 'Hartman-Hahn' condition, and to determine the 90°

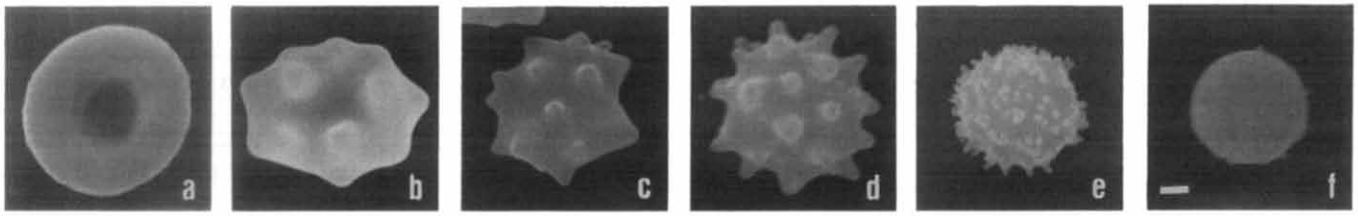

Fig. 1. Scanning electron micrograph of erythrocytes treated with MPPC or ethanol, yielding discocytes (a) and stage 1 to 5 echinocytes (b to f, respectively). The bar represents 1 μm.

pulse of ^{1}H and ^{13}C. Under these conditions the H_1 fields for ^{1}H and ^{13}C were 200.13 MHz and 50.33 MHz, respectively. Contact times were typically 2 ms. The chemical shift scale was relative to tetramethylsilane (Me_4Si, TMS). Peak assignment was according to Oldfield et al. [33]. Since the resonances arising from ^{13}C of phosphocholine headgroup do not show any appreciable shift upon addition of ethanol or MPPC, these peaks were used as internal references for the determination of relative change of hydrocarbon chain signals.

To convert ^{13}C-NMR chemical shift of hydrocarbon chains into a packing parameter of cell membranes, we calculate N_g, the average number of *gauche* bonds of fatty acyl hydrocarbon chains in the ghost membrane, as follows:

$$P_g = (35.4 - CS_m)/(35.4 - 28.5) \quad (4)$$

$$N_g = P_g \cdot 16 \quad (5)$$

where CS_m is the chemical shift (ppm) of methylene of lipids in the ghost membrane, P_g, the partition of *gauche* in acyl chains, is equal to the ratio of number of *gauche* to carbon numbers of the lipids (16-carbon chain-length was used in this calculation). Here, we assume the chemical shifts of all *gauche* and all *trans* methylenes of the membrane lipids to be 28.5 and 35.4 ppm, respectively. These two values were taken from cyclotetraeicosane crystal model studies [22]. The results using this method yield N_g numbers for DPPC dispersions comparable with those obtained by the Raman scattering method [34].

Results

Morphology and hemolysis studies

Human RBCs incubated with suspensions of MPPC or ethanol underwent shape change from discocytes to echinocytes. The stages of erythrocyte echinocytosis are demonstrated in Fig. 1. Fig. 2 shows the representative time courses of both the morphological changes and hemolysis of RBCs induced by MPPC (Fig. 2A) and ethanol (Fig. 2B). In the cases of MPPC-treated cells, the morphological index (MI) reached equilibrium within 5 min and was stable for the next 3 h. The same type of time course was observed for hemolysis when it occurred with a sufficiently high concentration of MPPC. In contrast, the ethanol-treated RBCs showed progressive increases in MI and hemolysis with time. The same time-dependent changes were observed for other short-chain alcohols such as butanol and hexanol. Fig. 3 summarizes the results of the concentration-dependence of the morphological change and hemolysis of

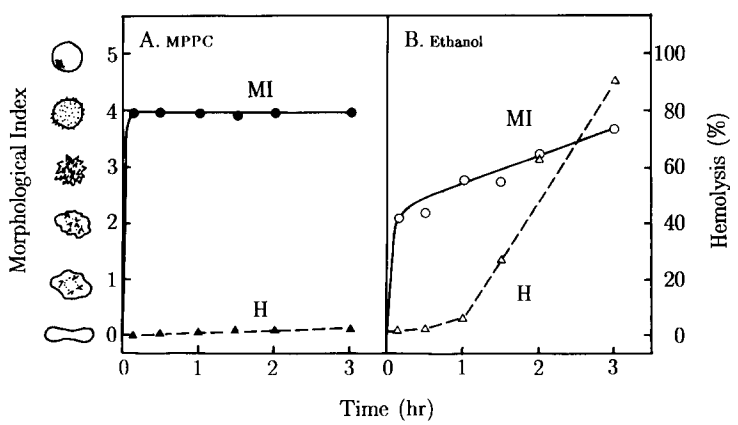

Fig. 2. Time courses of changes in morphology and hemolysis of red blood cells. RBCs at 2% hematocrit were incubated with (A) 3.8 μM of MPPC and (B) 3.4 M of ethanol. Morphological index (●, ○) and hemolysis (▲, △) were determined as described in Materials and Methods.

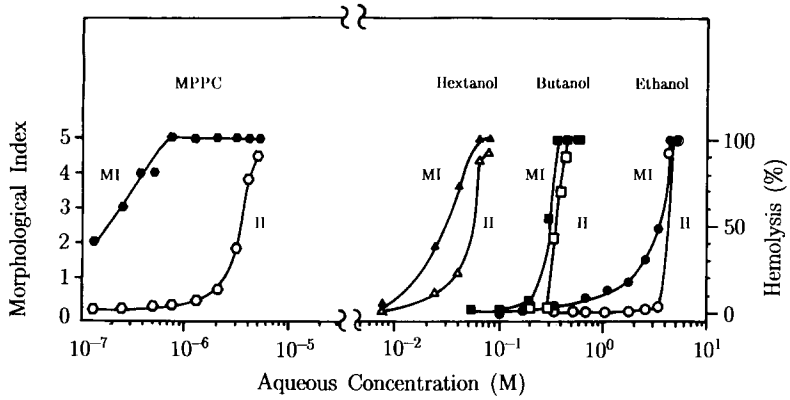

Fig. 3. Concentration dependence of changes in morphology and hemolysis of RBCs induced by short-chain alcohols and MPPC. RBCs at 2% hematocrit were incubated with different concentrations of ethanol (●, ○), 1-butanol (■, □), 1-hexanol (▲, △) and MPPC (⬣, ⬡) for 60 min, and then assessed for morphologic index (filled symbols) and % hemolysis (open symbols).

RBCs after 1-h incubation with various concentrations of MPPC and short-chain alcohols. Three points can be observed. First, the bulk concentrations needed to induce either morphological changes or hemolysis were several orders of magnitude higher for the alcohols than for MPPC. This difference can be attributed mainly to the differences in their partition coefficients and hence the membrane concentrations. When the data are plotted in terms of membrane concentrations, the various amphipaths give much closer results, as shown in Fig. 4. Second, the MPPC concentration needed to induce shape change and to cause hemolysis differ by approximately one order of magnitude, whereas these concentrations were close together for short-chain alcohols. The agreement between the morphology and hemolysis curves for short-chain alcohols was even better for studies performed at 2 or 3 h (data not shown). Third, the shorter the hydrocarbon chain of the exogenous molecule, the higher was the concentration needed to induce the same degree of shape change or hemolysis. This difference can again be attributed to the partition behavior of these molecules. Further evidence of the above argument is supported by the studies of morphological index and hemolysis of RBC as a function of hematocrit as well as MPPC concentration (data not shown). Using the methods described under Experimental Procedure and the previously obtained partition coefficient, i.e., $7.25 \cdot 10^4$ for MPPC and 0.14, 1.5, and 13 for ethanol, butanol and hexanol, respectively, one can calculate the amphipath concentrations needed for RBC to induce morphological and hemolytic changes (Fig. 4). To induce the same stage of morphological

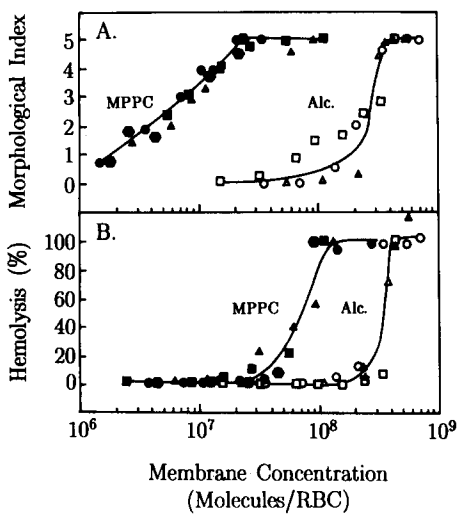

Fig. 4. Changes in morphology and hemolysis of RBCs as functions of membrane concentrations of MPPC and alcohols. Filled symbols are MPPC data for hematocrits at 0.01 (⬣), 0.2 (▲), 2 (■) and 50% (●). Open symbols are data for ethanol (○), 1-butanol (□) and 1-hexanol (△). Membrane concentrations were determined according to Eqn. 3.

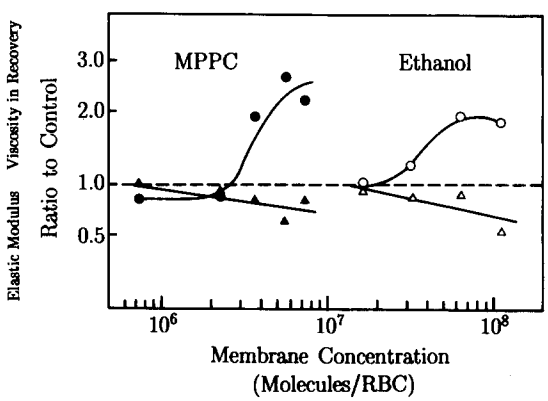

Fig. 5. Viscoelastic properties on MPPC- and ethanol-trated RBCs measured by micropipette aspiration. RBCs at 0.01% hematocrit were suspended in BSA-Tris buffer. The viscosity values (●, ○) and elastic moduli (▲, △) are expressed as the ratio of the value for MPPC- or ethanol-treated cells to the value for the control cells. Each data point consists of approx. 20 pairs of cells. Concentrations of MPPC in RBC have been calibrated according to the shape change curve in the presence and absence of BSA.

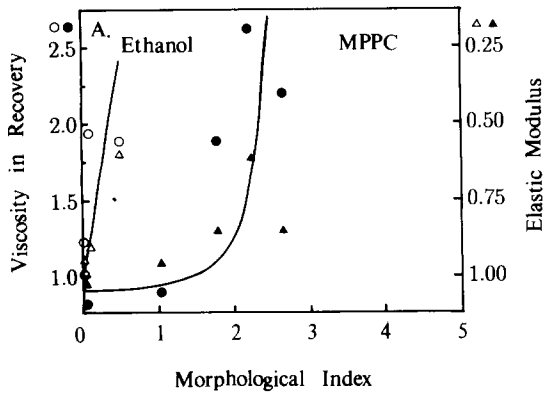

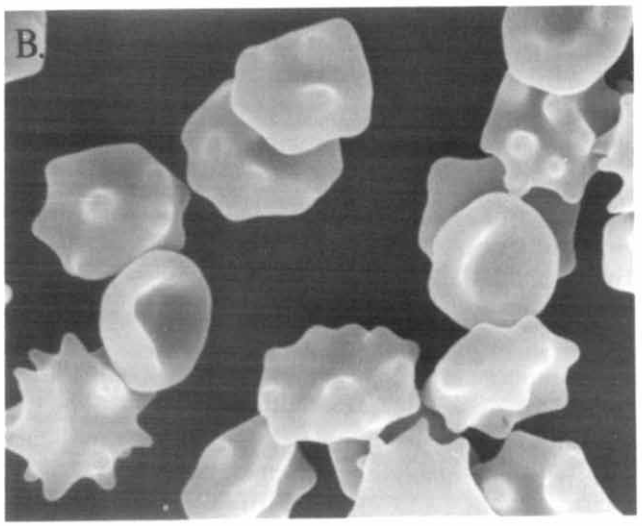

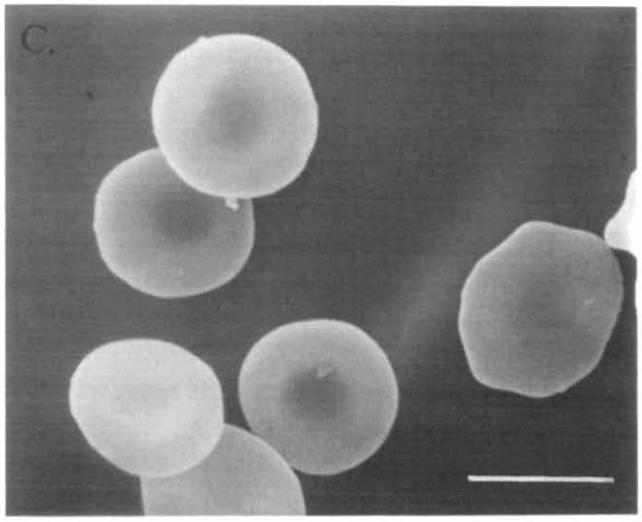

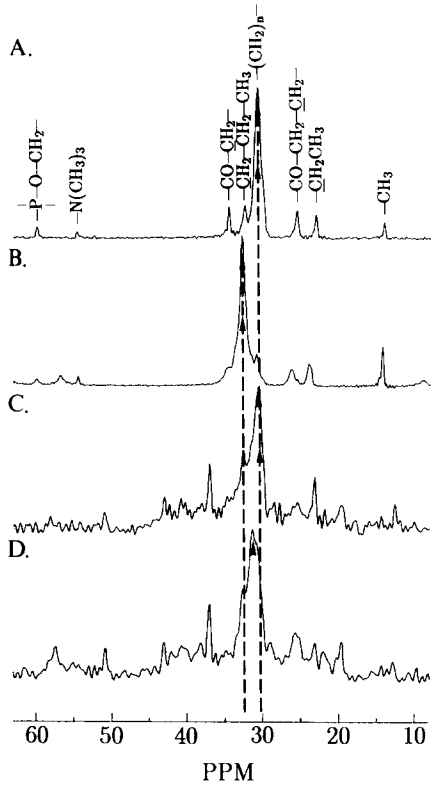

Fig. 7. 50.3 MHz CP/MAS ^{13}C-NMR spectra for (A) DPPC multilamellar dispersion at 43° C, (B) DPPC multilamellar dispersion at 25° C, (C) ethanol-treated ghosts at 25° C, (D) normal ghosts at 25° C. Chemical shift was related to tetramethylsilane. The arrows mark the peaks of methylene resonance for model and biological membranes.

change of RBC, e.g., for stage 3 echinocytes, the concentrations needed are $8 \cdot 10^6$ and $2.5 \cdot 10^8$ molecules/RBC for MPPC and short-chain alcohols, respectively ($\approx$ 30-fold difference). To induce 50% hemolysis, $7 \cdot 10^7$ and $3.5 \cdot 10^8$ molecules of MPPC and short-chain alcohols are needed, respectively ($\approx$ 5-fold difference).

Micropipette studies

The normal RBC membrane has three major structural components: the lipid bilayer, integral membrane proteins and cytoskeletal proteins [14,35]. By using the micropipette aspiration technique, viscoelasticity of individual RBC can be studied in detail. RBCs suspended in media without ethanol or MPPC treatment were determined as control, and the results on the treated cells were normalized by using the control experiments

Fig. 6. (A) Membrane viscoelastic moduli versus morphological index (MI) of RBCs treated with DPPC (closed symbols) and ethanol (open symbols). Values of viscosity index (circle) and elastic modulus (triangle) were taken from Fig. 5. Shapes of erythrocytes treated with (B) MPPC or (C) ethanol were viewed by scanning electron microscope for samples of RBCs exhibiting significant changes in viscoelastic properties. The bar represents 5 μm.

conducted on the same day. Typical values (mean ± S.D.) of membrane elastic modulus and viscosity in the recovery phase were determined to be $2.6(\pm 0.5) \cdot 10^{-3}$ dyn · cm^{-1} and $1.0(\pm 0.1) \cdot 10^{-4}$ dyn · s · cm^{-1}, respectively. As shown in Fig. 5, the elastic modulus decreased and viscosity of recovery phase increased with increasing concentrations of ethanol and MPPC. Values of phase I and phase II viscosity during deformation did not show any significant change (data not shown). In Fig. 6A, RBC membrane viscosity during recovery and elastic modulus are plotted as a function of cell morphology studied at the same concentrations of ethanol or MPPC. MPPC-treated cells exhibited significant changes in viscoelasticity only after stage 2 echinocyte formation (Fig. 6B). In contrast, ethanol-treated cells showed significant changes in viscoelasticity even with a minimal change in RBC shape (Fig. 6C).

NMR studies

Fig. 7 shows the representative ^{13}C-NMR spectra of (A) DPPC multilamellar dispersions at 43° C, (B) DPPC multilamellar dispersions at 25° C, (C) ethanol-treated ghost membranes and (D) normal ghost membranes. Since DPPC dispersions are known to show lipid phase transition at 41° C, changes of chemical shift for the main hydrocarbon chain from 25° C to 43° C are attributable to changes of the population of *trans-gauche* isomerization. One can thus infer the changes of *gauche* population by amphipathic agents from the changes in chemical shift of hydrocarbon chain from ghost membrane lipids. By using the method described in Eqn. 4, one can calculate the number of *gauche* (N_g) as a function of either ethanol or MPPC concentration in the ghost membrane (Fig. 8A). Since RBC underwent hemolysis at these concentrations, we correlated the degree of hemolysis with the number of *gauche* bonds for membrane lipids (Fig. 8B). It can be seen that N_g for ethanol is greater than N_g for MPPC at given levels of hemolysis.

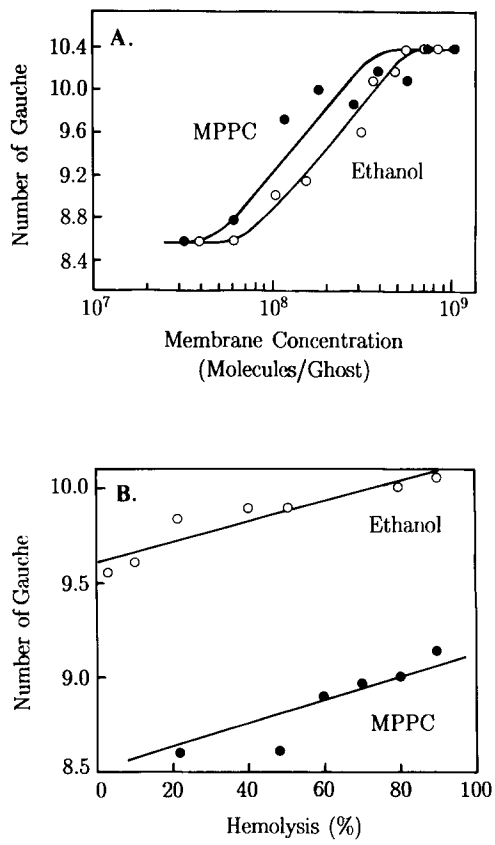

Fig. 8. (A) The average number of *gauche* bonds for fatty acid hydrocarbon chains on MPPC- and ethanol-treated ghost membranes. The number of *gauche* bonds was calculated from chemical shift changes of fatty acid hydrocarbons on MPPC- (●) or ethanol-treated (○) condensed ghost membrane by using Eqns. 4 and 5. (B) Relationship between the number of *gauche* bonds for fatty acyl chain of membrane lipids and the degree of hemolysis for MPPC- (●) and ethanol-treated (○) RBCs.

Discussion

In the present study, the effects of MPPC and three short-chain alcohols on RBC morphology and hemolysis were investigated, and the influences of MPPC and ethanol on membrane viscoelastic properties of single RBCs and lipid lateral packing density of RBC ghost membranes were studied. Quantitative comparisons between these amphipathic agents showed that the bulk concentrations required to induce changes in these morphological and biophysical parameters are several orders of magnitude lower for MPPC than for the short-chain alcohols and that the bulk concentrations required varied inversely with the molecular size of the alcohols. The differences among the three alcohols are almost entirely attributable to the variations in their partition coefficients, as the use of RBC membrane concentrations instead of bulk concentrations caused the results to come into close agreement. The difference between MPPC and the alcohols in causing shape change and hemolysis is also in large part attributable to the discrepancy in partition coefficient. The use of membrane concentration instead of bulk concentration markedly reduced the 4 to 6 orders of magnitude difference, but there is still a residual difference of 1 to 2 orders of magnitude. This indicates that MPPC and alcohols are different in their interactions with the RBC membrane in causing morphological changes and hemolysis. Another difference between MPPC and the alcohols is that MPPC induces morphologic changes at a much lower concentration than that needed to cause hemolysis. While morphologic changes also precede hemolysis for short-chain alcohols (Fig. 3), the discrepancies are much less than that observed for MPPC. It is known that lysophosphatidylcholine remains in the outer hemileaflet of intact RBCs, whereas ethanol can freely penetrate through the cell membrane [2,4,27]. Thus the

dramatic effect of short-chain alcohols on RBC shape can not be explained simply in terms of the asymmetric distribution of amphipaths between two hemileaflets of the bilayer [1].

Micropipette aspiration experiments indicate that MPPC and ethanol causes a decrease in membrane elastic modulus (Fig. 5), which is different from the effects of other echinocytic agents, e.g., sodium salicylate [35] which cause an increase, and benzylalcohol [16] which cause no change in elastic modulus. On the other hand, there are no significant differences in membrane mechanical properties between fresh biconcave and ATP-depleted crenated RBC [44,45]. Therefore, echinocytic shape cannot be simply correlated with membrane viscoelasticity. It is interesting that, concurrent with the decrease in elastic modulus, membrane viscosity during recovery increases in response to the amphipathic agents used in the present study. In general, membrane elastic modulus and viscosity tend to change in the same direction [41,42]. In hereditary spherocytosis, however, the RBCs do show a decrease in membrane elastic modulus with an increase in membrane viscosity [43]. Since these rheological changes in hereditary spherocytosis can be correlated with a decrease in membrane spectrin content [43], it is possible that the rheological effects of MPPC and ethanol may also be mediated by a change in cytoskeletal proteins through lipid–protein interactions. At the very high alcohol concentrations in the medium, mechanical changes of RBC have also been demonstrated as a result of changes in cytoskeletal protein structure [46].

It has been shown that the alterations of membrane deformability in shape-transformed RBCs can return to normal when either the echinocyte or stomatocyte recovers to become a biconcave discocyte [35]. Therefore, RBC morphology per se has an important relation to the membrane mechanical properties. This led us to cross plot the RBC membrane viscoelastic properties against the morphological index (Fig. 6A). Our results show that the rheology of ethanol-treated RBCs is greatly altered when they began to show shape change. The rheology of MPPC-treated RBCs, however, remains normal until significant formation of spicules (such as stage 2 echinocyte). This observation is consistent with our results that the echinocytic state of RBC induced by MPPC could remain stable without hemolysis (Fig. 3). Therefore, the shape transformation of ethanol-treated RBCs is closely associated with alternations in membrane viscoelastic properties, and this may play a role in the causing hemolysis.

Membrane fluidity has previously been studied extensively by electron spin resonance [36,37] and fluorescence techniques [38,39]. These techniques report the dynamics of the incorporated probe as an indicator of membrane properties and are sensitive to the local microenvironmental change around the exogenous probe molecules. Alterations in membrane fluidity can be detected by fluorescence depolarization without measurable changes in membrane viscoelasticity [16]. The NMR method used in the present study to determine the dynamics and packing of membrane, i.e., cross polarization/magic angle spinning (CP/MAS) ^{13}C-NMR, is different in several respects from other methods of fluidity measurements such as fluorescence anisotropy detection [16]. First, naturally abundant ^{13}C-NMR chemical shift is used as an indicator of the packing of fatty acyl hydrocarbon chain, and hence no external probe is needed [21]. Second, the chemical shifts of the hydrocarbon chain signals from all membrane lipids are followed, and hence ^{13}C-NMR provides information on the average property of the cell membrane, rather than the microenvironment around the probe. Hence, our present ^{13}C-NMR approach is less sensitive than the probe techniques and it may have a closer relationship to the macroscopic properties of the RBC membrane measured by micropipette aspiration. Third, ^{13}C-NMR chemical shift is a sensitive parameter for hydrocarbon chain conformation and packing density [22]. From our model membrane studies, the melting of DPPC dispersions will move the chemical shift of ^{13}C signals of hydrocarbon chains upfield by approx. 2 ppm (Fig. 7). It is known that the average surface areas of DPPC molecules in gel and liquid states are approx. 50 Å^2 and 60 Å^2, respectively [40]. Therefore 1 ppm chemical shift change is associated with 10% surface area expansion as estimated from model membrane studies. Since our detectable changes for ghost membrane treated with either ethanol or MPPC were up to 1 ppm, it suggests that our ^{13}C-NMR results reflect changes of lipid lateral packing. To interpret chemical shift as a useful physical parameters in membrane studies, we convert its value into number of *gauche* bonds, N_g. In general, the higher the N_g value, the lesser is the lipid lateral packing density, or the greater is the surface area expansion. According to previous Raman scattering and solid-state ^{2}H-NMR studies, the N_g value for gel and liquid states are different by approx. 7 units [34]. Our data on the differences of N_g between MPPC and ethanol induced hemolysis (see Fig. 8B) would correspond to about 15% of the total lipid lateral expansion observed during lipid phase transition. Therefore, in the concentration range studied, the surface areas of RBC membrane during MPPC- and ethanol-mediated hemolysis differ by approx. 1%. Although it is not clear whether 1% difference of the surface area expansion in these two systems could account for the detected differences in our results of morphological change and hemolysis of RBC, it certainly suggests that progressive changes in the lipid lateral packing are related to hemolysis.

The effects of MPPC and ethanol on the four types of measurements made in this study, via morphological

index, membrane viscoelasticity, number of *gauche* bonds, and hemolysis, can be summarized as follows. All these curves show a sigmoid relation with the membrane concentration of the amphipathic agents. For both agents, as the membrane concentration is raised, the increase in membrane viscosity precedes the change in the number of *gauche* bonds (a function of membrane surface area), and hemolysis correlates well with changes in lipid lateral packing. These results indicate that progressive changes in the molecular packing in the membrane, as detected by the two biophysical techniques, lead eventually to hemolysis. The parameter that behaves particularly differently in response to the two agents is the morphological index. While RBC morphological changes are very prominent at an MPPC concentration which causes only minimal membrane biophysical alterations, they are absent in ethanol-treated RBCs until the membrane concentration is raised to a level when membrane biophysical alterations have approached their maxima. These results indicate that the relationship between cell morphology and membrane biophysics is complex and it varies with the types of amphipaths, probably due to the different modes of amphipath interaction with the membrane.

In conclusion, MPPC and ethanol have been shown to be able to induce mrophological, hemolytic and biophysical changes of RBCs at certain critical membrane concentrations. MPPC elicits these changes at lower membrane concentrations than ethanol. While the shape change induced by ethanol is closely followed by membrane biophysical changes and hemolysis, the shape change induced by MPPC needs to be quite extensive before alterations in biophysical properties and hemolysis set in. These results provide insights into RBC membrane dynamics and serve to elucidate some of the interrelationship between RBC morphology and cell membrane properties.

Acknowledgments

This work was supported by the National Science Council, R.O.C. under grant NSC-77-0208-M007-92 and NSC-78-0412-B001-03. L.C. was a recipient of a predoctoral fellowship from N.S.C.

References

1 Sheetz, M.P. and Singer, S.J. (1974) Proc. Natl. Acad. Sci. USA 71, 4457–4461.
2 Lange, Y. and Slayton, J.M. (1982) J. Lipid Res. 23, 1121–1127.
3 Daleke, D.L. and Huestis, W.H. (1985) Biochemistry 24, 5406–5416.
4 Ferrell, J.E., Lee, K.-J. and Huestis, W.H. (1985) Biochemistry 25, 2849–2857.
5 Isomaa, B., Hägerstrand, H. and Paatero, G. (1987) Biochim. Biophys. Acta 899, 93–103.
6 Bütikofer, P., Brodbeck, U. and Ott, P. (1987) Biochim. Biophys. Acta 901, 291–295.
7 Klibansky, C. and De Vries, A. (1963) Biochim. Biophys. Acta 70, 176–187.
8 Lange, Y., Gough, A. and Steck, T.L. (1982) J. Membr. Biol. 69, 113–123.
9 McLawhon, R.W., Marikovsky, Y., Thomas, N.J. and Weinstein, R.S. (1987) J. Membr. Biol. 99, 73–78.
10 Ferrell, J.E. and Huestis, H.W. (1984) J. Cell Biol. 98, 1992–1998.
11 Weltzien, H.U. (1979) Biochim. Biophys. Acta 559, 259–287.
12 Katsu, T., Ninomiya, C., Kuroko, M., Kobayashi, H., Hirota, T. and Fujita, Y. (1988) Biochim. Biophys. Acta 939, 57–63.
13 Bierbaum, T.J., Bouma, S.R. and Huestis, W.H. (1979) Biochim. Biophys. Acta 555, 102–110.
14 Waugh, R.E. (1987) Biophys. J. 51, 363–369.
15 Reinhart, W.H. and Chien, S. (1986) Blood 67, 1110–1118.
16 Chabanel, A., Abbott, R.E., Chien, S. and Schachter, D. (1985) Biochim. Biophys. Acta 816, 142–152.
17 Chien, S. (1987) Annu. Rev. Physiol. 49, 177–192.
18 Seelig, J. and Seelig, A. (1980) Q. Rev. Biophys. 13, 19–61.
19 Balchelor, J.G. and Prestegard, J.H. (1972) Biochem. Biophys. Res. Commun. 48, 70–75.
20 Braach-Maksvytis, V.L.B. and Cornell, B.A. (1988) Biophys. J. 53, 839–843.
21 Oldfield, E., Meadows, M., Rise, D. and Jacobs, R. (1978) Biochemistry 17, 2727–2740.
22 Saitô, H. (1986) Magn. Reson. Chem. 24, 835–852.
23 Bessis, M. (1973) in Red Cell Shape; Physiology, Pathology, Ultrastructure (Bessis, M., Weed, R.I. and Leblond, P.F., eds.), pp. 1–24, Springer-Verlag, Heidelberg.
24 Lieber, M.R., Lange, Y., Weinstein, R.S. and Steck, T.L. (1984) J. Biol. Chem. 259, 9225–9234.
25 Chi, L.-M. and Wu, W. (1990) Biophys. J. 57, in press.
26 Dodge, J.T., Mitchell, C. and Hanahan, D.J. (1963) Arch. Biochem. Biophys. 100, 119–130.
27 Seeman, P. (1972) Pharmacol. Rev. 24, 583–655.
28 Chien, S., Sung, K.-L.P., Skalak, R., Usami, S. and Tözeren, A. (1978) Biophys. J. 24, 463–487.
29 Hanahan, D.J. and Ekholm, J.E. (1974) Methods Enzymol. 31, 168–180.
30 Seeman, P., Roth, S. and Schneider, H. (1971) Biochim. Biophys. Acta 225, 171–184.
31 Maciel, G.E. (1984) Science 226, 282–288.
32 Ackerman, S.K., Noguchi, C.T., Schechter, A.N. and Torchia, D.A. (1982) Biochem. Biophys. Res. Commun. 106, 1161–1168.
33 Oldfield, E., Bowers, J.L. and Forbes, J. (1987) Biochemistry 26, 6919–6923.
34 Pink, D.A., Green, T.J. and Chapman, D. (1980) Biochemistry 19, 349–356.
35 Chabanel, A., Reinhart, W. and Chien, S. (1987) Blood 69, 739–743.
36 Rubenstein, J.L.R., Smith, B.A. and McConnell, H.M. (1979) Proc. Natl. Acad. Sci. USA 76, 15–18.
37 Presti, F.T. and Chan, S.I. (1982) Biochemistry 21, 3821–3830.
38 Lentz, B.R., Barenholz, Y. and Thompson, T.E. (1976) Biochemistry 15, 4521–4528.
39 Lentz, B.R., Barrow, D.A. and Hoechli, M. (1980) Biochemistry 19, 1943–1954.
40 Silver, B.L. (1985) in Physical Chemistry of Membranes, pp. 35–55, the Solomon Press, New York.
41 Sung, K.-L.P., Freedman, J., Chabanel, A. and Chien, S. (1985) Br. J. Haematol. 61, 455–466.
42 Chabanel, A., Sung, K.-L.P., Rapiejko, J., Prchal, J.T., Palek, J., Liu, S.C. and Chien, S. (1989) Blood 73, 592–595.
43 Waugh, R.E. and Agre, P. (1988) J. Clin. Invest. 81, 133–141.
44 Meiselman, H.J., Evans, E.A. and Hochmuth, R.M. (1978) Blood 52, 499–504.
45 Baker, R.F. (1982) Blood Cells 7, 551–558.
46 Vertessy, V.G. and Steck, T.L. (1989) Biophys. J. 55, 255–262.